Analysis of the Effect of Electrode Variation and Current on the Welding Results of Corten A Steel using SMAW Method on Microstructure, Corrosion Resistance, and Mechanical Properties

Mavindra Ramadhani [*], Rochman Rochiem, Muhammad Irsyad Zain
[1]Materials and Metallurgical Department, Faculty of Industrial Technology and System Engineering,
Institut Teknologi Sepuluh Nopember, Surabaya
Email: mavindra@its.ac.id[*]

Received: 2023-05-09 Received in revised from: 2023-05-17 - Accepted: 2023-05-17

Abstract

The emission exhaust stack in industries must have good corrosion resistance and heat resistance in both the base metal and the welded joints. Therefore, corten steel is chosen as the base metal for the exhaust stack due to its excellent corrosion resistance and heat resistance, as well as its costeffectiveness compared to other heat-resistant steels. This study aims to analyze the welded joints of corten steel in terms of microstructure, corrosion resistance, and tensile strength using the Shielded Metal Arc Welding (SMAW) method, following the Welding Procedure Specification (WPS). The variables used in this study are the electrode variations using E7016-G and E8016-G electrodes, and the current variations of 90, 105, and 120 A. The results of this study indicate that in the metallography testing, the highest percentage of the perlitic phase is found in specimen B2, which uses the E8016-G electrode and a current of 105A, reaching 41.92% in the weld metal and 29.6% in the Heat-Affected Zone (HAZ). In the corrosion resistance testing, the corrosion rate fluctuates within the 3-hour and 6-hour time ranges, but decreases within the 10-hour time range. The lowest corrosion rate is observed in specimen B2 using the E8016-G electrode and a current of 105A. In terms of mechanical properties, the best results are obtained from the tensile testing and hardness testing of specimen B2 using the E8016-G electrode and a current of 105A.

Keywords: *Current; Corten A steel; Electrode; SMAW*

1. Introduction

The emission exhaust stack on the Barge Mounted Power Plant (BMPP) vessel at PT. PAL Indonesia (Persero) is made of rolled and welded corten steel sheets. This exhaust stack operates at a temperature of 374°C. Corten steel has good high-temperature corrosion resistance, but the welded joints may not necessarily exhibit the same properties. According to the American Welding Society (AWS), the chosen electrode should have properties and composition that are at least similar to the base metal used. The corten steel used in the exhaust stack has a tensile strength of 70 ksi, so it requires a welding electrode with equivalent tensile strength, such as the E7016-G electrode. In addition to electrode selection, the magnitude of the current used can also affect the properties of the welded joints. According to Ghazvinloo [1], the welding current used can affect the mechanical properties of the welded joints. However, it is important to ensure that the current used during the welding process remains in accordance with the Welding Procedure Specification (WPS). This specification provides guidelines and standards for welding processes, including the appropriate range of current to be used to achieve desired weld quality and mechanical properties. Adhering to the WPS helps maintain consistency and ensures that the welded joints meet the required specifications.

Several previous studies on welding corten steel have yielded various conclusions. Based on the research by Deepak James Raj et al. [2], it was concluded that when welding corten steel using an ER70S-6 electrode, certain important elements evaporate during the welding process. These elements are necessary for corten steel to exhibit its desired heat resistance and corrosion resistance properties.

Another study by Deepak James Raj et al. [3] concluded that welding corten steel using an electrode containing Cu-Cr-Ni resulted in better mechanical properties and improved corrosion resistance compared to electrodes without these elements. In a previous study on the influence of current on Shielded Metal Arc Welding (SMAW) welding results by Santoso et al. [4], it was concluded that higher welding currents used in the SMAW process can provide better mechanical properties and affect the microstructure of the welded joints. These studies highlight the importance of electrode selection, the presence of specific alloying elements, and the influence of welding current on the properties of welded corten steel joints. It is crucial to consider these factors to achieve the desired performance and durability in welding applications involving corten steel. The choice of electrode and welding current used in the SMAW process for welding corten steel can indeed affect the weld results. Corten steel contains additional elements such as copper (Cu), chromium (Cr), and nickel (Ni), so the electrode used for this steel must also contain these elements while maintaining a tensile strength above 70 ksi. The E8016-G electrode is often compared to the E7016-G electrode in this regard. Furthermore, the selection of welding current is also crucial in achieving good mechanical properties. In this case, currents of 90, 105, and 120 A are used to determine the current that produces satisfactory weld results. Therefore, further research is needed to explore the influence of electrode selection and welding current on the welding outcomes of corten steel. This will help to determine the optimal parameters for achieving desired weld quality, mechanical properties, and overall performance in corten steel welding applications.

2. Method

This article discusses the variation in electrodes and current in the welding results of corten A steel using the SMAW process, focusing on the microstructure, corrosion resistance, and mechanical properties. The variations used include the use of E7016-G and E8016-G electrodes with currents of 90, 105, and 120 A. In this study, corten A (weathering steel) is used as the base metal for welding, with dimensions of 300 x 100 mm and a thickness of 6 mm. Corten A is a High Strength Low Alloy (HSLA) steel known for its excellent atmospheric corrosion resistance [3]. The composition and mechanical properties of corten A steel can be seen in Table 1 and Table 2, respectively.

Table 1. Chemical Composition of Corten A Steel

Element	Composition (%)
Carbon (C)	< 0,19 Max
Manganese (Mn)	0,8 – 1,25
Phosphorus (P)	0,04 Max
Sulfur (S)	0,05 Max
Silicon (Si)	0,3 – 0,65
Chrome (Cr)	0,4 – 0,65
Nickel (Ni)	0,4 Max
Vanadium (V)	0,02 – 0,1
Copper (Cu)	0,25 – 0,4
Iron (Fe)	*Balanced*

Table 2. Mechanical Properties of Corten A Steel

Ultimate Tensile Strength	Yield Strength	Elongation	Hardness
483 MPa	338 MPa	23,10%	158 HV

The selection of electrodes depends on various factors, one of which is the chemical composition and properties of the metal to be welded. Welding electrodes should ideally have the same composition

and properties as the base metal. However, typically, welding electrodes actually have higher composition and better properties compared to their base metal. This is because certain elements are lost during the welding process, which can lead to a decrease in properties [5]. The composition, classification, and mechanical properties of E7016-G and E8016-G electrodes can be seen in Table 3, Table 4, and Table 5.

Table 3. Electrode Composition

Electrode	Element	Composition (%)
EXX16-G[a]	Carbon (C)	-
	Manganese (Mn)	1 min[b]
	Phosfor (P)	0,03
	Sulfur (S)	0,03
	Silicon (Si)	0,8 min[b]
	Chrome (Cr)	0,3 min[b]
	Nickel (Ni)	0,5 min[b]
	Vanadium (V)	0,1 min[b]
	Copper (Cu)	0,2 min[b]

[a] The letters "XX" are used to represent the tensile strength level (70, 80, 90, 100, 110, 120 ksi) of the welding electrode. [b] To meet the requirements of Group G electrodes, the unwelded base metal must contain at least one element from the following Table 4.

Table 4. Electrode Classification

Electrode	The coating type of the electrode	Welding position	Current type
EXX16-G[a]	Low hydrogen potassium	Flat, Vertikal, Over head, Horizontal	AC or DCEP

[a] The letters "XX" are used to represent the tensile strength level (70, 80, 90, 100, 110, 120 ksi) of the welding electrode.

Table 5. Electrode Mechanical Properties

Electrode	Tensile strength	Yield Strength	Elongation (%)
E7016-G	490 MPa	390 MPa	22%
E8016-G	550 MPa	460 MPa	19%

The welding process is performed using the Shielded Metal Arc Welding (SMAW) method. Welding is carried out according to the parameters specified in the Welding Procedure Specification (WPS). The welding parameters used and the test piece diagram can be seen in Table 6 and Figure 1 below. The tests conducted in this study are metallographic testing, high-temperature corrosion testing, and tensile testing.

Table 6. Welding Parameters

Parameters	Value
Voltage (V)	20

Ampere (A)	90, 105, dan 120
Travel Speed (mm/min)	84
Heat Input (kJ/mm)	1,51
Electrode	E7016-G, dan E8016-G
Groove (˚)	60
Max Pass Thickness (mm)	3
Root Spacing (mm)	2,4
Position	3G (Uphill)
Polarity	DCEP

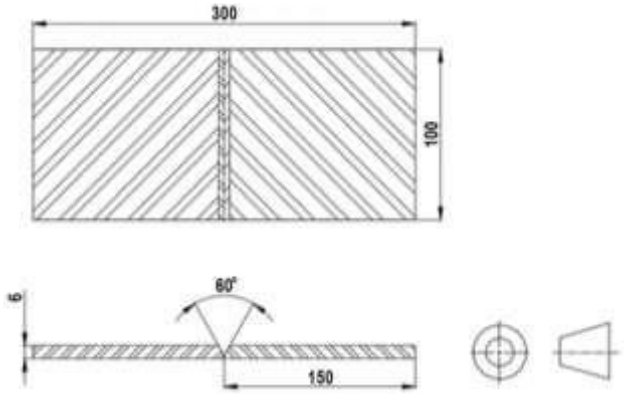

Figure 1. Test Piece

3. Results and Discussion

In the metallographic testing, microstructure images were captured using a microscope at a magnification of 50 times. The microstructure images of all specimens can be seen in Figure 2, Figure 3, Figure 4, Figure 5, Figure 6, and Figure 7 below.

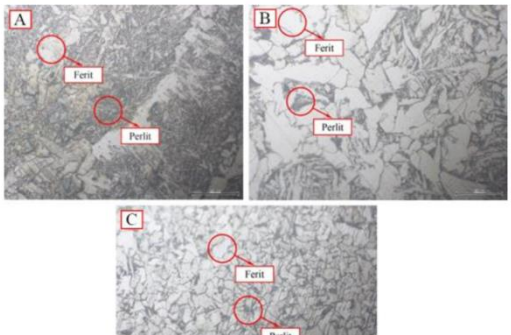

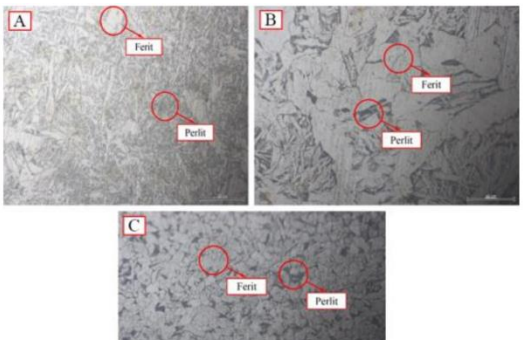

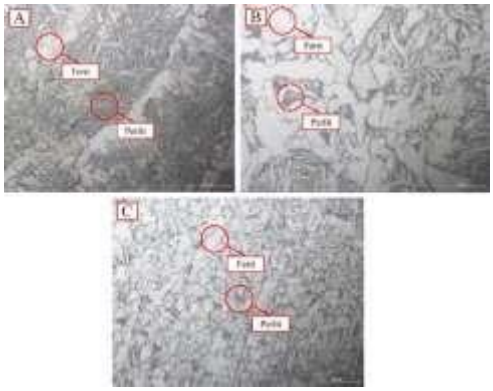

Figure 2. Microstructure of Specimen A1
(A) Weld Metal, (B) HAZ, (C) Base Metal

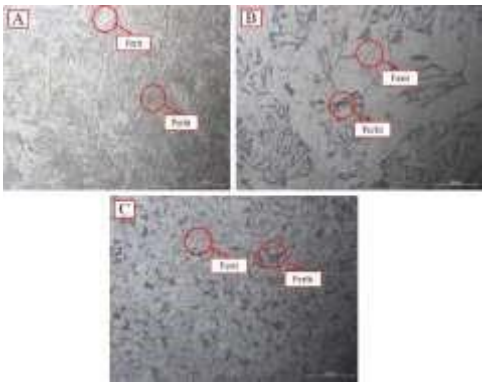

Figure 3. Microstructure of Specimen A2
(A) Weld Metal, (B) HAZ, (C) Base Metal

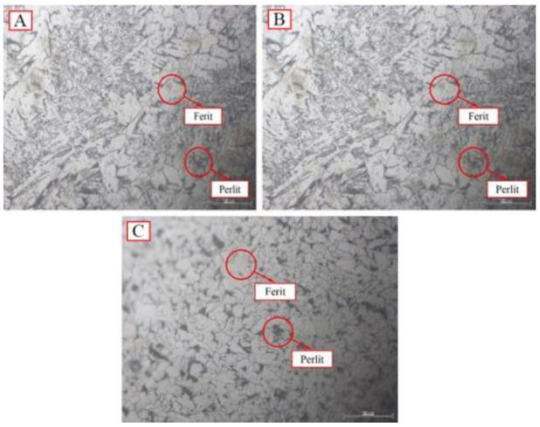

Figure 4. Microstructure of Specimen A3
(A) Weld Metal, (B) HAZ, (C) Base Metal

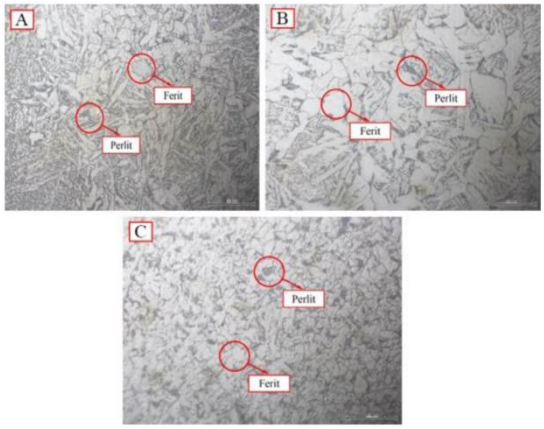

Figure 5. Microstructure of Specimen B1
(A) Weld Metal, (B) HAZ, (C) Base Metal

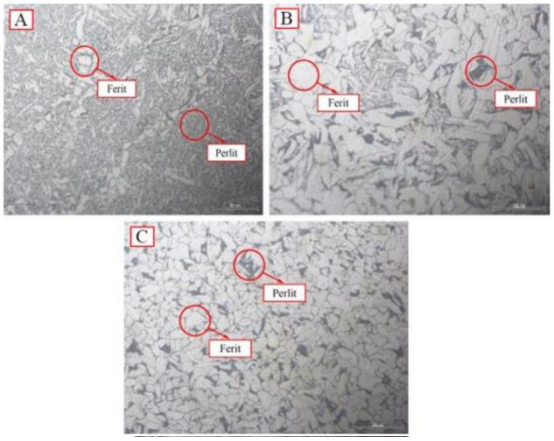

Figure 6. Microstructure of Specimen B2
(A)Weld Metal, (B) HAZ, (C) Base Metal

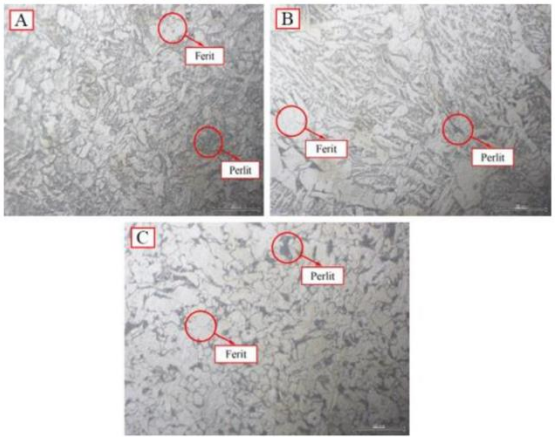

Figure 7. Microstructure of Specimen B3
(A) Weld Metal, (B) HAZ, (C) Base Metal

Based on the microscope images, two phases are observed in all specimens in three areas: perlite phase (black) and ferrite phase (white). Subsequently, phase percentage calculations were performed on all specimens in the three areas using the ImageJ application. The phase percentage ratios can be seen in Table 8 below.

Tabel 8. Phase Precentage

Specimen	Phase Precentage (%)

	Weld Metal		HAZ		Base Metal	
	Ferrite	Perlite	Ferrite	Perlite	Ferrite	Perlite
A1	68,43	31,57	74,95	25,05	77,93	22,07
A2	63,05	36,95	72,34	27,66	78,19	21,81
A3	69,67	30,33	76,9	23,1	77,96	22,04
B1	62,35	37,65	73,12	26,88	77,43	22,57
B2	58,08	41,92	70,4	29,6	77,59	22,41
B3	66,02	33,98	74,29	25,71	77,33	22,67

According to Table 8, the percentage of perlite phase tends to increase in the weld metal and HAZ areas. The percentage of perlite also increases from specimen A1 to A2 but decreases in specimen A3 in the weld metal and HAZ areas. In specimen B2, there is an increase and a decrease in specimen B3 in the weld metal and HAZ areas. Specimen B also shows an increase in perlite phase compared to specimen A. The highest percentage of perlite phase in the weld metal and HAZ areas is found in specimen B2 with a perlite phase percentage of 41.92% in the weld metal area and 29.6% in the HAZ area. The lowest percentage of perlite phase in the weld metal and HAZ areas is found in specimen A3 with a perlite phase percentage of 30.33% in the weld metal area and 23.1% in the HAZ area. In the base metal area, the percentage of perlite phase tends to be the same because it is not directly affected by the welding process, ranging from 21.81% to 22.67%.

The microstructure and the amount of phase formed in the weld metal and HAZ areas are influenced by the current magnitude used. This is because different current settings can affect the heat input into the welded metal during the welding process, resulting in different cooling rates. These different cooling rates can affect the microstructure formed in the welded metal. In the base metal area, there is no change in the microstructure because it is not directly exposed to the heat cycles of the welding process, thus tending to maintain the same microstructure as before welding [6]. The use of welding electrodes with different tensile strengths, such as E7016-G and E8016-G, can affect the amount of perlite phase formed in the weld metal and HAZ areas. The higher the tensile strength value of the electrode used, the more perlite will appear in both areas. The formation of perlite phase in the weld metal and HAZ areas occurs due to the trapping of carbon in the fusion zone during the cooling process by the surrounding air [7].

In the high-temperature corrosion testing, the initial and final masses of the specimens were measured after being subjected to a muffle furnace, and the corrosion rate (weight loss) was calculated using a specific formula. The results of this testing can be seen in Table 9, and the comparison of corrosion rates can be observed in Figure 8 below.

Table 9. Corrosion Rate Value Data for Each Specimen

Time (Hour)	Specimen	Change in mass (mg)	Corrosion rate (mpy)
3	*Base metal*	2,3	9,329

	A1	0,7	2,987
	A2	0,8	3,732
	A3	0,5	2,246
3	B1	0,8	3,515
	B2	0,4	1,666
	B3	0,9	3,901
6	*Base metal*	3,4	7,441
	A1	3,2	7,06
	A2	1,7	3,719
	A3	2	4,247
6	B1	0,9	2,047
	B2	0,7	1,512
	B3	2,4	5,252
10	*Base metal*	4,3	0,006
	A1	2,8	0,004
	A2	2,3	0,003
	A3	2,5	0,003
10	B1	3,1	0,004
	B2	3,2	0,004
	B3	3,7	0,005

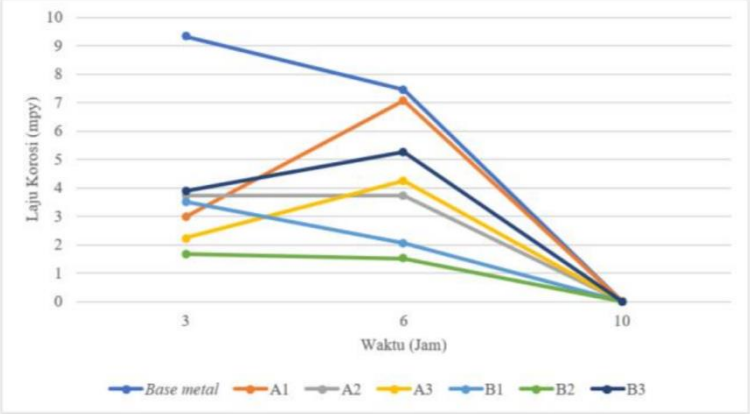

Figure 8. Corrosion Rate Comparison Graph Against Time

Based on Table 9 and Figure 8 above, the corrosion rates of all specimens tend to fluctuate at 3 hours and 6 hours, but all specimens show a decrease in corrosion rate at 10 hours. The lowest corrosion rate is observed in specimen B2 at 3 hours and 6 hours, while the highest corrosion rate is observed in the base metal at 3 hours and 6 hours. The decrease in corrosion rate is attributed to the formation of a protective oxide layer on the specimen's surface. This oxide layer is formed due to the presence of elements such as copper, chromium, and nickel, which react to form oxides. Additionally, the corrosion rate can also be influenced by the fineness of the phase grains, as a finer grain structure tends to decrease the corrosion rate [8]. Weathering steel (Corten A steel) forms two oxide layers. The inner layer of Corten

A steel is compact, crack-free, and acts as a protective barrier against corrosion, thereby enhancing the corrosion resistance of the metal. This inner oxide layer is formed by phosphorus, which strengthens the oxide layer in Corten A steel that has a high phosphorus content
[9].

In the tensile testing, values for Ultimate Tensile Strength (UTS), yield strength, and elongation were obtained from the stress-strain curve. The results of this testing can be seen in Table 10, and the comparison of UTS and yield strength values can be observed in Figure 9 below.

Tabel 10. Tensile Testing Results Data

Specimen	Tensile Testing Results		
	UTS(N/mm^2)	*Yield Strength* (N/mm^2)	*Elongation* (%)
A1	491,53 ±17,06	421,66 ± 4,34	24,11 ± 0,18
A2	515,43 ± 7,96	455,98 ± 7,31	24,15 ±0,59
A3	501,41± 12,57	444,25 ± 8,98	17,00 ± 1,85
B1	543,94 ± 8,51	479,03 ± 3,31	16,52 ± 0,58
B2	550,45 ± 4,84	486,49 ± 5,08	16,79 ± 0,79
B3	491,73 ± 29,1	437,82 ± 14,67	13,85 ± 2,70

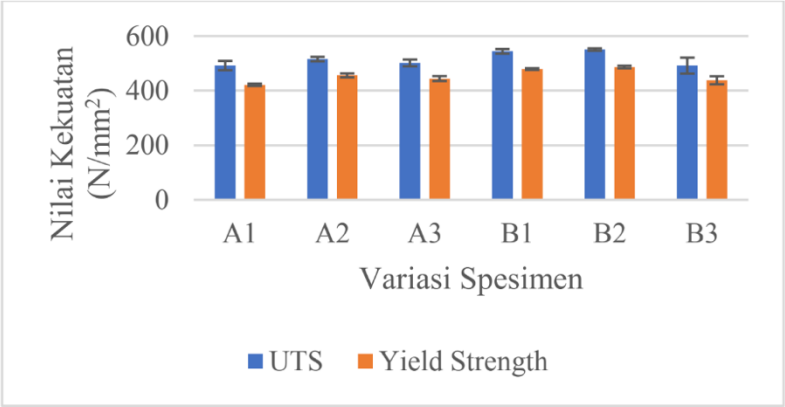

Figure 9. UTS dan Yield Strength Comparison Chart

Based on Table 10 and Figure 9 above, the highest values for tensile strength and yield strength in specimen A were obtained from specimen A2. The elongation values in specimen A at 90A and 105A currents were relatively similar, but there was a decrease when using the 120A current. Similarly, in specimen B, the highest tensile strength and yield strength values were obtained from specimen B2, which used a 105A current. The elongation values in specimen B at 90A and 105A currents were also relatively similar, but there was a decrease when using the 120A current. The highest UTS and yield strength values were obtained by specimen B2, with values of 550.45 N/mm^2 for UTS and 486.49 N/mm^2 for yield strength. The lowest UTS and yield strength values were obtained by specimen A1, with values of 491.53 N/mm^2 for UTS and 421.66 N/mm^2 for yield strength. The highest elongation value was obtained by specimen A2, with a value of 24.15%, while the lowest elongation value was obtained by specimen B3, with a value of 13.85%. The choice of current can influence the tensile strength of the welded joints. The use of a 105A current results in better tensile strength and yield strength because the 105A current provides more stable welding conditions compared to the 90A and 120A currents in the Shielded Metal Arc Welding (SMAW) method. A stable current leads to a good arc, ensuring sufficient

heat to melt the electrode and the test material, resulting in a well-fused joint [10]. The selection of electrodes can also affect the tensile strength of the welded joints. Specimen B tends to have higher tensile strength compared to specimen A because the E8016-G electrode has higher tensile strength and yield strength compared to the E7016-G electrode. This means that using the E8016-G electrode will result in higher tensile strength compared to using the E7016-G electrode [11].

In the hardness testing, hardness values were obtained for three areas: weld metal, HAZ (HeatAffected Zone), and base metal. The results of this testing can be seen in Table 11, and the comparison of hardness values can be seen in Figure 10 below.

Tabel 11. Hardness Test Result Data

Specimen	Hardness Value Vickers (HV)		
	Weld Metal	HAZ	Base Metal
A1	248,33 ± 5,03	222,67 ± 4,16	207,00 ± 1,00
A2	260,00 ± 4,36	229,33 ± 2,08	208,00 ± 2,65
A3	228,67 ± 4,73	212,67 ± 0,58	208,67 ± 1,53
B1	281,33 ± 5,86	232,33 ± 2,08	208,33 ± 2,08
B2	295,00 ± 5,29	240,33 ± 7,57	207,67 ± 1,53
B3	246,33 ± 6,03	228,67 ± 4,93	208,33 ± 1,53

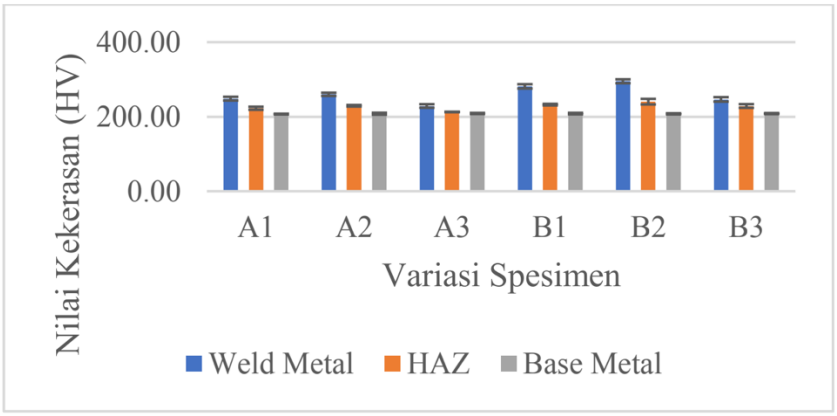

Figure 10. Hardness Comparison Chart

Based on Table 11 and Figure 10 above, the highest hardness values in the weld metal and HAZ were obtained from specimen B2, with a hardness value of 295 HV for the weld metal and 240.33 HV for the HAZ. The lowest hardness values in the weld metal and HAZ were obtained from specimen A3, with a hardness value of 228.67 HV for the weld metal and 212.67 HV for the HAZ. The hardness values in the base metal area tended to be similar for each specimen, ranging from 207 HV to 208.67 HV. It can also be observed that the hardness decreases from the weld metal to the HAZ, and further to the base metal. This is due to the difference in the amount of perlite phase present in each region, where a higher content of perlite phase can increase the hardness of the material. Perlite phase contributes to hardness because it contains lamellar cementite, which has hard and strong properties [12]. In specimen A, an increase in hardness can be seen from specimen A1 to specimen A2, and a decrease in hardness from specimen A2 to specimen A3. This is also attributed to the difference in the phases present in each specimen. Specimen A2 has the highest amount of perlite phase among the specimens, resulting in the highest hardness among the specimens in group A. Specimen B exhibits similar trends to specimen A. The hardness value of specimen B2 is the highest among specimens B1 and B3. This is because specimen B3 has a higher content of perlite phase compared to other specimens in group B. In all current settings,

specimens B have higher hardness values compared to specimens A. This is also influenced by the use of E8016-G electrode in welding, which results in a higher content of perlite phase compared to the use of E7016-G electrode, leading to increased hardness in the weld metal and HAZ regions. In addition to being influenced by the percentage of perlite phase, the welding current can also affect the melting temperature of the electrode. Using the appropriate current setting ensures good electrode melting and HAZ area coverage, thus maximizing the hardness of the welded metal. Using currents that are too low or too high can result in poor electrode melting and insufficient or excessive HAZ coverage, leading to decreased hardness [13].

4. Conclussion

Conclusion from the analysis and discussion are as follows: In the metallography test, an increase in the percentage of perlite phase was observed in the weld metal and HAZ areas compared to the base metal. The highest increase in perlite phase was found in specimen B2, which used the E8016-G electrode and a current of 105A, reaching 41.92% in the weld metal and 29.6% in the HAZ. The lowest percentage of perlite phase was found in specimen A3, which used the E7016-G electrode and a current of 120A, with a perlite phase percentage of 30.33% in the weld metal and 23.1% in the HAZ. The base metal had relatively similar percentages of perlite phase in all specimens.

In the corrosion resistance test, it was found that the corrosion rate was fluctuating within the 3-hour and 6-hour time range, which was due to different rates of oxide formation on each specimen. However, the corrosion rate decreased within the 10-hour time range. The best corrosion resistance was observed in specimen B2, which used the E8016-G electrode and a current of 105A, with corrosion rates of 1.666 mpy at 3 hours, 1.512 mpy at 6 hours, and 0.004 mpy at 10 hours. In the tensile strength test, an improvement was observed from using a current of 90A to 105A, but a decrease was observed at 120A for both specimen A and B. Tensile strength also increased from using the E7016-G electrode to the E8016-G electrode. In the hardness test, an increase was observed in the weld metal and HAZ areas compared to the base metal. The hardness values also increased from using a current of 90A to 105A but decreased at 120A for both specimen A and B. The hardness values also increased from using the E7016-G electrode to the E8016-G electrode. The specimen B2, which used the E8016-G electrode and a current of 105A, exhibited the best mechanical properties based on the tensile test and hardness test, with a tensile strength of 550.45 N/mm^2, yield strength of 486.49 N/mm^2, elongation of 16.79%, hardness of 295.00 HV in the weld metal, and hardness of 240.33 HV in the HAZ.

Reference

[1] H. R. Ghazvinloo and N. Shadfar, "Effect of arc voltage , welding current and welding speed on fatigue life , impact energy and bead penetration of AA6061 joints produced by robotic MIG welding," no. February, 2010.

[2] J. R. Deepak, V. K. Bupesh Raja, P. Viswanatha Reddy, L. Lakshmi Venkata Sai, and G. Ashok Kumar Reddy, "Investigation of microstructural and metallurgical properties of corten A588 grade steel gtaw joints," *Int. J. Mech. Prod. Eng. Res. Dev.*, vol. 9, no. 5, pp. 1257–1264, 2019, doi: 10.24247/ijmperdoct2019111.

[3] D. J. Raj, V. K. B. Raja, T. S. Savan, and S. Babu, "Development of novel tricoated CuNiCr filler for welding weathering steel," *AIP Conf. Proc.*, vol. 2311, no. December, 2020, doi: 10.1063/5.0034619.

[4] T. B. Santoso, Solichin, and P. T. Hutomo, "Pengaruh Kuat Arus Listrik Pengelasan Terhadap Kekuatan Tarik Dan Struktur Mikro Las Smaw Dengan Elektroda E7016," *J. Tek. Mesin*, vol. 15, no. 1, p. 20, 2015.

[5] American Welding Society. Committee on Filler Metals and Allied Materials., American National Standards Institute., and American Welding Society. Technical Activities Committee., "Specification for stainless steel electrodes for shielded metal arc welding." p. 42, 2014.

[6] S. Mizhar and I. H. Pandiangan, "Pengaruh Masukan Panas Terhadap Struktur Mikro, Kekerasan dan Ketangguhan pada Pengelasan Shielded Metal Arc Welding (SMAW) dari Pipa Baja Diameter 2,5 inch," *J. Din.*, vol. II, no. 14, pp. 16–22, 2014.

[7] Y. Winardi, F. Fadelan, M. Munaji, and W. N. Krisdiantoro, "Pengaruh Elektroda Pengelasan Pada Baja AISI 1045 Dan SS 202 Terhadap Struktur Mikro Dan Kekuatan Tarik," *J. Pendidik. Tek. Mesin Undiksha*, vol. 8, no. 2, p. 86, 2020, doi: 10.23887/jptm.v8i2.27772.

[8] M.- Rohmah, "Pengaruh Penempaan Dan Perlakuan Panas Terhadap Sifat Mekanik Dan Ketahanan Korosi Pada Modifikasi Baja Laterit a-588," *Metalurgi*, vol. 36, no. 1, p. 33, 2021, doi: 10.14203/metalurgi.v36i1.579.

[9] F. I. Wei, "Atmospheric corrosion of carbon steels and weathering steels in Taiwan," *Br. Corros. J.*, vol. 26, no. 3, pp. 209–214, 1991, doi: 10.1179/000705991798269215.

[10] Y. N. I. Saputro, "Pengaruh Arus Pengelasan Terhadap Kekuatan Tarik Sambungan Las Smaw Dengan Elektroda E 7018," *J. Kaji. Teknol.*, vol. 13, no. 2, pp. 24–31, 2011.

[11] J. Arifin, H. Purwanto, and I. Syafa'at, "Pengaruh Jenis Elektroda Terhadap Sifat Mekanik Hasil Pengelasan," *Momentum*, vol. 13, no. 1, pp. 27–31, 2017.

[12] D. Juliaptini, "Skripsi Analisis Sifat Mekanik dan Metalografi Baja Karbon Rendah untuk Aplikasi Tabung Gas 3 Kg," *Skripsi*, pp. 1–90, 2015.

[13] A. S. Mohruni and B. H. Kembaren, "Pengaruh Variasi Kecepatan Dan Kuat Arus Dengan Elektroda E6013," *J. REKAYASA MESIN*, vol. 13, no. 1, pp. 1–8, 2013.